9. W. O. Milligan and R. H. Morriss, *J. Am. Chem. Soc.* **86**, 3461 (1964).
10. B. Bruche, *Kolloid-Z.* **170**, 97 (1960).
11. A. C. Curtis *et al.*, *Angew. Chem. Int. Ed. Engl.* **27**, 1530 (1988).
12. D. G. Duff, P. P. Edwards, B. F. G. Johnson, *J. Phys. Chem.* **99**, 15934 (1995).
13. L. D. Rampino and F. F. Nord, *J. Am. Chem. Soc.* **63**, 2745 (1942).
14. A. Henglein, B. G. Ershov, M. Marlow, *J. Phys. Chem.* **99**, 14129 (1995).
15. T. S. Ahmadi *et al.*, in preparation.
16. A. I. Kirkland, P. P. Edwards, D. A. Jefferson, D. G. Duff, *Annu. Rep. Prog. Chem. Sect. C* **87**, 247 (1990).
17. We thank the Office of Naval Research (grant N00014-95-1-0306) for its financial support of this project.

12 December 1995; accepted 25 April 1996

A Benzene-Thermal Synthetic Route to Nanocrystalline GaN

Yi Xie, Yitai Qian,* Wenzhong Wang, Shuyuan Zhang, Yuheng Zhang

A thermal reaction of Li_3N and $GaCl_3$ in which benzene was used as the solvent under pressure has been carried out for the preparation of 30-nanometer particles of gallium nitride (GaN) at 280°C. This temperature is much lower than that of traditional methods, and the yield of GaN reached 80%. The x-ray powder diffraction pattern indicated that sample was mainly hexagonal-phase GaN with a small fraction of rocksalt-phase GaN, which has a lattice constant a = 4.100 angstroms. This rocksalt structure, which had been observed previously only under high pressure (at least 37 gigapascals) was observed directly with high-resolution electron microscopy.

Hexagonal GaN with the wurtzite structure is a direct band-gap semiconductor with wide band gap (3.39 eV at room temperature) (*1*). It has potential applications in light-emitting devices in the visible to ultraviolet region (*2*). GaN with the rocksalt structure has been detected previously with energy-dispersive x-ray-diffraction for samples prepared in diamond-anvils. The phase that forms at ultrahigh pressure (≥37 GPa) disappeared as the pressure was released (*3*).

Johnson *et al.* (*4*) first prepared hexagonal GaN through the following reaction at temperatures above 900°C:

$$2Ga + 2NH_3 \rightarrow 2GaN + 3H_2$$

Usually, powder samples of hexagonal GaN were synthesized by placing some source materials such as $GaCl_3$ or $Ga(CH_3)_3$ under flowing ammonia at temperatures from 600° to 1000°C (*5*). Recently, precursors such as $[H_2GaNH_2]_3$ or $Ga(C_2H_5)_3NH_3$, which already have a Ga–N bond, could be pyrolysized to produce GaN at relatively low temperatures, but posttreatment temperatures >500°C are needed (*6*).

Nitrides of lanthanide and transition metals (M) can be synthesized through solid-state metathesis reactions such as:

$$MCl_n + Li_3N \rightarrow MN + LiCl$$

in the temperature range from 600 to 1100°C (*7*). However, the reaction of $GaCl_3$ with Li_3N through a similar process for the preparation of GaN failed (*8*).

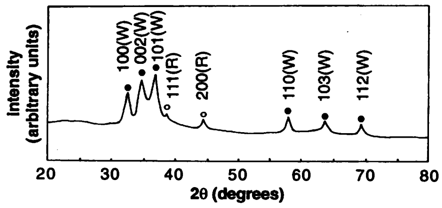

Fig. 1. An XRD pattern of nanocrystalline GaN.

We report on the reaction of Li_3N with $GaCl_3$ in benzene at 280°C under pressure in an autoclave. Nanocrystalline GaN was produced through what may be a liquid-solid reaction:

$$GaCl_3 + Li_3N \xrightarrow{\text{benzene}} GaN + 3LiCl$$

We call this technique a benzene thermal process, which is similar to a hydrothermal process, except that benzene is substituted for water.

In order to ensure the quality of the chemical reagent, Li_3N (*9*) and anhydrous $GaCl_3$ (*10*) were synthesized according to previously reported methods.

An appropriate amount of $GaCl_3$ solution in benzene and Li_3N powder was put into a silver-liner stainless steel autoclave of 50-ml capacity, and then the autoclave was filled with benzene up to 75% of the total volume. The air dissolved in the solution was driven off by passing argon gas through the solution. The autoclave was maintained at 280°C for 6 to 12 hours and then allowed to cool to room temperature. A dark-gray precipitate was collected that was washed with absolute ethanol to remove LiCl. The final product was dried in vacuum at 100°C for 2 hours.

The x-ray powder diffraction (XRD) pattern was recorded on a Japan Rigaku Dmax γA x-ray diffractometer with CuKα radiation (λ = 1.54178 Å). In the XRD pattern (Fig. 1), reflections marked with dots can be indexed to the hexagonal cell of GaN with lattice constants *a* = 3.188 Å and *c* = 5.176 Å, which are near the reported values (*11*). However, an unusually strong (002) peak in the pattern indicates a preferential orientation of [001] in nanocrystalline GaN. Other small reflections (marked with circles) can be indexed to cubic GaN in rocksalt structure with *a* = 4.100 Å, which is greater than the reported value of 4.006 Å at 50 GPa (*3*). The curve of volume versus pressure (*3*) shows that the

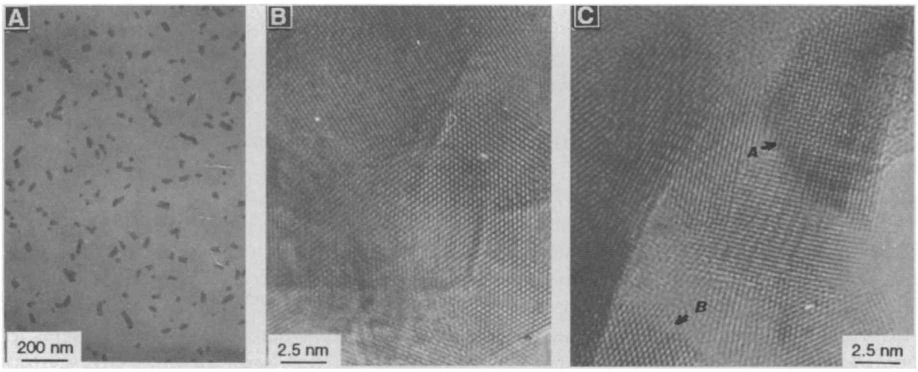

Fig. 2. (**A**) A TEM micrograph of nanocrystalline GaN. (**B** and **C**) HREM images of nanocrystalline GaN: (B) Lattice fringes of (001) plane in GaN with a wurtzite structure and (C) lattice fringes of (100) and (110) planes in GaN (marked A and B, respectively) with a rocksalt structure.

Y. Xie and Y. Qian, Structure Research Laboratory and Department of Applied Chemistry, University of Science and Technology of China, Hefei, Anhui 230026, People's Republic of China.
W. Wang, Department of Applied Chemistry, University of Science and Technology of China, Hefei, Anhui 230026, People's Republic of China.
S. Zhang and Y. Zhang, Structure Research Laboratory, University of Science and Technology of China, Hefei, Anhui 230026, People's Republic of China.

*To whom correspondence should be addressed.

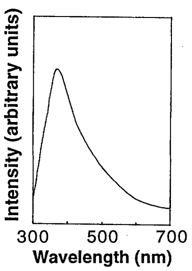

Fig. 3. Photoluminescence spectra of nanocrystalline GaN.

cell volume increases as pressure decreases; the lattice parameter was estimated to be 4.035 Å at 37 GPa.

Transmission electron microscopy (TEM) images were taken with a Hitachi H-800 transmission electron microscope. These crystallites of GaN have an average size of 32 nm and display a uniform shape (Fig. 2A). High-resolution electron microscopy (HREM) images of GaN particles were taken on a JEOL-2010 transmission electron microscope. In Fig. 2B, the (001) lattice fringes of GaN in the wurtzite structure appear frequently, indicating the preferential orientation of the platelike GaN particles. The areas marked by arrowheads (A and B) in Fig. 2C represent a typical structural image of [100] and [110] orientations, respectively, of GaN in the rocksalt structure.

Photoluminescence (PL) spectra of the nanocrystalline GaN were measured in a Hitachi 850 fluorescence spectrophotometer with a Xe lamp at room temperature. The excitation wavelength was 254 nm, and the filter wavelength was 310 nm. The PL spectrum (Fig. 3) consists of one broad emission feature at 370 nm, which is in agreement with that of the bulk GaN (*12*). This result indicates that the as-prepared GaN is too large for quantum confinement, and in fact the Bohr exciton radius for GaN is 11 nm, which could be calculated according to (*13*).

REFERENCES AND NOTES

1. R. Dingle and K. L. Shaklee, *Appl. Phys. Lett.* **19**, 5 (1971).
2. R. S. Schmitt *et al.*, *Phys. Rev. B* **35**, 8113 (1987).
3. H. Xia, Q. Xia, A. L. Ruoff, *ibid.* **47**, 12925 (1993).
4. W. C. Johnson, J. B. Parsons, M. C. Crew, *J. Phys. Chem.* **36**, 2561 (1932).
5. A. Addamiano, *J. Electrochem. Soc.* **108**, 1072 (1961); Z. A. Munir and A. W. Searcy, *J. Chem. Phys.* **42**, 4223 (1965); I. G. Pichugin and D. A. Searcy, *Inorg. Mater.* **6**, 1732 (1970); B. J. Isherwood and D. K. Wickenden, *J. Mater. Sci.* **5**, 869 (1970); E. Ejder, *J. Cryst. Growth* **22**, 44 (1974); T. Ogino and M. Aoki, *Jpn. J. Appl. Phys.* **18**, 1049 (1979); D. Elwell *et al.*, *J. Cryst. Growth* **66**, 45 (1984).
6. J. W. Hwang *et al.*, *Chem. Mater.* **7**, 517 (1995); J. E. Andrews and M. A. Littlejohn, *J. Electrochem. Soc.* **122**, 1273 (1975).
7. J. B. Wiley and R. B. Kaner, *Science* **255**, 1093 (1992).
8. J. C. Fitzmaurice and A. Hector, *Polyhedron* **13(2)**, 235 (1994).
9. J. C. Bailer, Ed. *Inorganic Syntheses* (McGraw-Hill, New York, 1955), vol. 4, p. 1.
10. H. S. Booth, Ed., *Inorganic Syntheses* (McGraw-Hill, New York, 1939), vol. 1, p. 26.
11. P. Perlin, C. J. Carillon, J. P. Itie, A. S. Miguel, *Phys. Rev. B* **45**, 83 (1992).
12. H. P. Maruska and J. J. Tietjent, *Appl. Phys. Lett.* **15**, 327 (1969).
13. B. K. Ridley, *Quantum Process in Semiconductors* (Clarendon Press, Oxford, 1982), pp. 62–66.
14. Supported by the Chinese National Foundation of Natural Science Research.

15 February 1996; accepted 4 April 1996

Experimental Constraints on Recycling of Potassium from Subducted Oceanic Crust

Max W. Schmidt*

Petrological experiments on oceanic crust samples characterize the recycling of potassium from mid-ocean ridge basalts and sediments. Metasomatism could develop directly and continuously from subducted potassium-bearing crust from shallow levels to a maximum depth of 300 kilometers. Phengite (a potassium-rich mica) is the principal potassium host at subsolidus conditions. It transports potassium and water to depths of up to 300 kilometers and could yield over the entire depth range potassium-rich fluids or melts (depending on the specific geotherm), which are likely to constitute one of the primary metasomatic agents for generation of calc-alkaline magmas.

Continental crust is growing mainly through calc-alkaline magmatism, which is related to destructive plate boundaries. Calc-alkaline magmatism from volcanic arcs is generally considered to form through partial melting of the mantle wedge after it has been fluxed with fluids or melts (*1*–*3*). These metasomatic fluids or melts carry water, potassium, and other large ion lithophile (LIL) elements such as Rb, Ba, Sr, and Th. Concentrations and isotopic compositions of U, Th, Pb, B, and Be in calc-alkaline magmas reflect derivation from subducted oceanic crust and sediments (*1*) and indicate that the metasomatic agent originated from the subducted slab (*4*). A systematic increase of K in volcanic arc magmas is commonly observed with increasing depth of subduction zones below arc volcanoes [the so-called K-depth relation (*5*)]. In most cases, this relationship is accompanied by a systematic increase in the abundance of trace elements such as the light rare earth elements (LREEs), Hf, Zr, Nb, Th, U, and Pb (*6*, *7*). In this paper, I use a series of experiments to explain the mechanism for transporting K_2O to depth and to understand the generation of K-rich metasomatic fluids.

I performed 51 experiments on mid-ocean ridge basalts (MORB) and andesite bulk compositions (*8*) (Table 1 and Fig. 1). For experiments at pressures above 4.0 GPa, I used a MA-8 multianvil apparatus. The assemblage was composed of prefabricated pyrophyllite gaskets, MgO-octahedra with an edge length of 18 mm, and a stepped graphite heater. Temperature gradients were 20° to 40°, pressure was accurate to ±4%. For experiments below 4.0 GPa, I used an end-loaded piston cylinder with a full salt assembly. Run times of 24 to 38 hours for the multianvil experiments (relatively high pressures and temperatures) and 200 to 350 hours for the piston cylinder experiments (relatively low pressures and temperatures) were necessary to produce almost homogeneous phases, only garnets preserved cores of relict seed compositions. Run products were analyzed by electron microprobe; the presence of small quantities of melt was determined by secondary electron microscopy.

In MORB, andesite [or greywacke (*8*)] (Fig. 1), the principal K-bearing phase observed at subsolidus conditions was phengite (a white mica). It formed at low pressures (<1.5 GPa) and remained present until 9.5 to 10.0 GPa (750° to 1050°C, Fig. 1). In the experiments, the silica content of

Table 1. Basaltic (KMB) and andesitic (RPR) starting material compositions (*8*) and averages (av) for MORB (*22*) and greywackes (GW) (*23*).

	KMB	av-MORB	RPR	av-GW
SiO_2	50.59	50.53	59.55	66.70
TiO_2		1.56	0.71	
Al_2O_3	18.96	15.27	16.97	13.50
Fe_2O_3	1.81		2.01	1.60
FeO	8.24	10.46	4.10	3.50
MnO			0.11	
MgO	6.93	7.47	3.18	2.10
CaO	10.08	11.49	6.55	2.50
Na_2O	2.90	2.62	2.86	2.90
K_2O	0.49	0.16	2.44	2.00
Total	100.00	99.69	99.36	94.80

Bayerisches Geoinstitut, 95440 Bayreuth, Germany

*Present address: CNRS-URA10, 5 rue Kessler, 63038 Clermont-Ferrand, France. E-mail: max@opgc.univ-bpclermont.fr